

SUPPLEMENTAL FILE 1

Model structures.

The model part that describes the relation between receptor activity and growth is largely phenomenological. In order to see what complexity is needed to describe this pathway, the following model structures were compared with respect to model complexity, data fit and predictive power:

Model 1. single stimulation, double inhibition (equation 5 in used for modelling root growth in main manuscript)

$$R(\text{BR}_{\text{I tot}}, \text{BL}_{\text{tot}}, t) = R(0,0,t) + \frac{E_{\text{max}}(t) * [\text{BR}_{\text{I BL}}]}{k_1 + [\text{BR}_{\text{I BL}}]} \frac{k_2}{k_2 + [\text{BR}_{\text{I BL}}]} \frac{k_3}{k_3 + [\text{BR}_{\text{I BL}}]}.$$

Model 2. double stimulation, double inhibition

$$R(\text{BR}_{\text{I tot}}, \text{BL}_{\text{tot}}, t) = R(0,0,t) + \frac{E_{\text{max}}(t) * [\text{BR}_{\text{I BL}}]}{k_1 + [\text{BR}_{\text{I BL}}]} \frac{[\text{BR}_{\text{I BL}}]}{k_4 + [\text{BR}_{\text{I BL}}]} \frac{k_2}{k_2 + [\text{BR}_{\text{I BL}}]} \frac{k_3}{k_3 + [\text{BR}_{\text{I BL}}]}.$$

Model 3. double stimulation, single inhibition

$$R(\text{BR}_{\text{I tot}}, \text{BL}_{\text{tot}}, t) = R(0,0,t) + \frac{E_{\text{max}}(t) * [\text{BR}_{\text{I BL}}]}{k_1 + [\text{BR}_{\text{I BL}}]} \frac{[\text{BR}_{\text{I BL}}]}{k_2 + [\text{BR}_{\text{I BL}}]} \frac{k_3}{k_3 + [\text{BR}_{\text{I BL}}]}.$$

Model 4. single stimulation, single inhibition (equation 7 used for modelling hypocotyl elongation in main manuscript)

$$R(\text{BR}_{\text{I tot}}, \text{BL}_{\text{tot}}, t) = R(0,0,t) + \frac{E_{\text{max}}(t) * [\text{BR}_{\text{I BL}}]}{k_1 + [\text{BR}_{\text{I BL}}]} \frac{k_2}{k_2 + [\text{BR}_{\text{I BL}}]}.$$

Model 5. single stimulation

$$R(\text{BR}_{\text{I1 tot}}, \text{BL}_{\text{tot}}, t) = R(0,0,t) + \frac{E_{\text{max}}(t) * [\text{BR}_{\text{I1 BL}}]}{k_1 + [\text{BR}_{\text{I1 BL}}]}$$

Model 6. single inhibition

$$R(\text{BR}_{\text{I1 tot}}, \text{BL}_{\text{tot}}, t) = R(0,0,t) + \frac{E_{\text{max}}(t) * k_1}{k_1 + [\text{BR}_{\text{I1 BL}}]}.$$

Model 7. triple stimulation, double inhibition

$$R(\text{BR}_{\text{II tot}}, \text{BL}_{\text{tot}}, t) = R(0,0,t) + \frac{E_{\text{max}}(t) * [\text{BR}_{\text{II BL}}]}{k_1 + [\text{BR}_{\text{II BL}}]} \frac{[\text{BR}_{\text{II BL}}]}{k_2 + [\text{BR}_{\text{II BL}}]} \frac{[\text{BR}_{\text{II BL}}]}{k_3 + [\text{BR}_{\text{II BL}}]} \frac{k_4}{k_4 + [\text{BR}_{\text{II BL}}]} \frac{k_5}{k_5 + [\text{BR}_{\text{II BL}}]}$$

Model 8. double stimulation, triple inhibition

$$R(\text{BR}_{\text{II tot}}, \text{BL}_{\text{tot}}, t) = R(0,0,t) + \frac{E_{\text{max}}(t) * [\text{BR}_{\text{II BL}}]}{k_1 + [\text{BR}_{\text{II BL}}]} \frac{[\text{BR}_{\text{II BL}}]}{k_2 + [\text{BR}_{\text{II BL}}]} \frac{k_3}{k_3 + [\text{BR}_{\text{II BL}}]} \frac{k_4}{k_4 + [\text{BR}_{\text{II BL}}]} \frac{k_5}{k_5 + [\text{BR}_{\text{II BL}}]}$$

Model 9. triple stimulation, triple inhibition

$$R(\text{BR}_{\text{II tot}}, \text{BL}_{\text{tot}}, t) = R(0,0,t) + \frac{E_{\text{max}}(t) * [\text{BR}_{\text{II BL}}]}{k_1 + [\text{BR}_{\text{II BL}}]} \frac{[\text{BR}_{\text{II BL}}]}{k_2 + [\text{BR}_{\text{II BL}}]} \frac{[\text{BR}_{\text{II BL}}]}{k_3 + [\text{BR}_{\text{II BL}}]} \frac{k_4}{k_4 + [\text{BR}_{\text{II BL}}]} \frac{k_5}{k_5 + [\text{BR}_{\text{II BL}}]} \frac{k_6}{k_6 + [\text{BR}_{\text{II BL}}]}$$

Model 10. single stimulation, triple inhibition

$$R(\text{BR}_{\text{II tot}}, \text{BL}_{\text{tot}}, t) = R(0,0,t) + \frac{E_{\text{max}}(t) * [\text{BR}_{\text{II BL}}]}{k_1 + [\text{BR}_{\text{II BL}}]} \frac{k_2}{k_2 + [\text{BR}_{\text{II BL}}]} \frac{k_3}{k_3 + [\text{BR}_{\text{II BL}}]} \frac{k_4}{k_4 + [\text{BR}_{\text{II BL}}]}$$

Model 11. triple stimulation, single inhibition

$$R(\text{BR}_{\text{II tot}}, \text{BL}_{\text{tot}}, t) = R(0,0,t) + \frac{E_{\text{max}}(t) * [\text{BR}_{\text{II BL}}]}{k_1 + [\text{BR}_{\text{II BL}}]} \frac{[\text{BR}_{\text{II BL}}]}{k_2 + [\text{BR}_{\text{II BL}}]} \frac{[\text{BR}_{\text{II BL}}]}{k_3 + [\text{BR}_{\text{II BL}}]} \frac{k_4}{k_4 + [\text{BR}_{\text{II BL}}]}$$

Here $R(0,0,t)$ is the root length at time point t without BR signaling, $E_{\text{max}}(t)$ is the maximum root length at time point t , $[\text{BR}_{\text{II BL}}]$ is the concentration of BR_{II} occupied by ligand and k_1, k_2, k_3, k_4, k_5 and k_6 are the half maximum response values. For all models it was assumed that there is still a small amount (0.1 nM of total BRs, simplified to BL only) present in the roots after addition of BRZ.

The different model structures were compared using the Akaike information criterion (AIC) and the Bayesian information criterion (BIC).

$$\text{AIC} = S(\theta) + 2p + \frac{2p(p+1)}{n-p-1} \quad [\text{S1}]$$

$$\text{BIC} = S(\theta) + p \log(n) \quad [\text{S2}]$$

These two error criteria are based on the weighted residual sum of squares $S(\theta)$ obtained from the parameter estimation (Supplemental File S2), the total

number of parameters to be estimated (p) and the number of data points (n). The main difference between the AIC and BIC criterion is that the BIC penalizes the number of free parameters p more (Klipp et al., 2009).

In the roots, models with only one module (models 5 and 6), or with less than two inhibitory modules (models 3, 4 and 11) have a significantly higher AIC and BIC scores, as well as a higher fitting error, clearly indicating a minimal necessary model complexity (Supplemental Table S1). Incorporation of at least one stimulatory module and two inhibitory modules is optimal for modelling the effect of BL on root growth. Incorporation of more than 2 stimulatory or more than 2 inhibitory modules (models 7, 8 and 9) can give similar AIC and BIC numbers as models 1 and 2. To make a well-founded model selection, the predictive power with respect to the *bri-116* null mutant was also taken into account. From the models 1, 2, 7, 8 and 9, model 1 gives the best prediction and was therefore selected.

In the hypocotyl, only one inhibitory module is required for a good fit (Supplemental Table S3). Models with one module in total still have significantly higher AIC and BIC scores. Similar to the situation in roots, the predictive power was taken into account for model selection. The differences between the models are smaller than for the models tested for the root data. However, since model 4 has the second lowest AIC score and the best prediction, this model was selected.

SUPPLEMENTAL FILE 2

Parameter estimation.

The unknown parameters $R(0,0,t)$, $E_{\max}(t)$, and the k values are estimated using a controlled random search algorithm (CRS; Price et al., 1976) and a hybrid algorithm consisting of two runs of the Matlab global search algorithm called Genetic Algorithm, followed by the Matlab gradient based search algorithm `lsqnonlin`. Both algorithms yielded similar parameter estimates (Table S2). Here the object function and the CRS method are discussed.

The maximum likelihood estimate in equation [4] is obtained by minimizing the object function:

$$S(\theta) = \sum_i \left(\frac{R(\text{BRI1}_{\text{tot}}, \text{BL}_{\text{tot}}(i), t, \theta) - R_i}{\sigma_i} \right)^2, \quad [\text{S3}]$$

where i is the index over the BL concentrations, $R(\text{BRI1}_{\text{tot}}, \text{BL}_{\text{tot}}(i), t, \theta)$ the predicted root lengths at time t for concentrations $\text{BL}_{\text{tot}}(i)$, based on the initial parameter vector θ , R_i the measured root lengths, and σ the standard deviation of assumed normally distributed noise on the data points. The main idea behind this algorithm is that, starting with an initial collection of parameter vectors, CRS repeatedly draws a new parameter vector that replaces a vector in the collection if its corresponding data fit is better. The CRS method starts by taking a random set of n_Q parameter vectors inside a search domain D and continues by computing the corresponding values of the object function. The bounds of D represent the *a priori* limits for the parameters. From this list of n_g vectors, a new vector is chosen using the rule

$$\theta_{\text{new}} = 2\bar{\theta}_{\text{rand}} - \theta_{\text{rand}} \quad [\text{S4}]$$

where θ_{rand} is a random vector from the list, and $\bar{\theta}_{\text{rand}}$ is the average of a random subset of p vectors in the list. To ensure that the new vectors are selected with equal preference over the logarithmic space, [S4] is modified element wise to

$$\theta_{\text{new}} = 10^{\log(2\bar{\theta}_{\text{rand}}) - \log(\theta_{\text{rand}})}. \quad [\text{S4}]$$

If $S(\theta_{\text{new}}) < \max(S(\theta))$, and $\theta_{\text{new}} \in D$, the parameter vector with the maximum object function is replaced by the new one:

$$\theta | \{S(\theta) = \max(S(\theta))\} \rightarrow \theta_{\text{new}}.$$

By repeating this, the worst fitting parameter vectors are removed continuously and replaced by ones with a better fit. Eventually, the points will form a cloud that gets denser and denser. The algorithm stops when

$$\max(\mathbf{S}(\theta)) \leq s_c \cdot \min(\mathbf{S}(\theta)) \quad [\text{S5}]$$

with s_c the stop criterion. So the worst fit has an at most $100(s_c - 1)$ % larger

S value than that of the best fit. We used the following values: $s_c=1.0001$,

$n_Q=800$, and $D=[10^{-3}, 10^3]$ for each parameter.

SUPPLEMENTAL FILE 3

The k values are altered in BRI1-GFP reporter lines.

The model is not able to predict the behaviour of the BRI1-GFP reporter lines. Only a decrease in the half maximum response values can explain the increased sensitivity of these lines. There are two possible causes for an altered half maximum response value. First, a rate limiting component can be out titrated, thereby making these lines hypersensitive to the ligand. Second, there can be a higher residual BL concentration after BRZ treatment in the BRI1-GFP reporter lines, when compared to the Col-0 lines. The latter will result in a stronger response of the lines towards exogenously applied BL. To ensure that this is not due to a higher level of leftover endogenous BL after BRZ treatment, measurements were repeated with a BRZ concentration of 5 μM instead of 1 μM (Fig. S11). Although this further reduced the root length of the BRI1-GFP reporter lines, the model was still not able to predict the behaviour of the BRI1-GFP reporter lines. Therefore, predicted decrease in k value in these lines is likely due to shortage of a negative regulator.

SUPPLEMENTAL FILE 4

Supplementary Materials and Methods.

Plant lines and growth conditions

In the root growth assays, the homozygous *bri1-116* and *bri1-201* lines were scored on the cabbage phenotype on 20-day-old seedlings. To evaluate if there was a difference between wild type and the heterozygous pool of *bri1-116* and *bri1-201*, only the non-cabbaged plants were taken into account. As proof of principle, individual plants (n=25 plants) were genotyped to confirm the plant was homozygous or heterozygous for the mutation. Genotyping was performed by PCR using the following primer combinations: *bri1-201* mutant forward (TCAAGCTTCTGTAAACA) or *bri1-201* wild type forward (GCTTCTTTCTCTGTAAAC)/ BRI1-LRR reversed (GGAGATTGATTGCAGAAAGATCCAG). Genotyping of the *bri1-116* line was done by PCR amplification using the following primer combination: forward (CGAATCACTCGCGTTGTGAGTAACAAC)/ reversed (CCAACTCCGCCTTTTCTTTCTCC) followed by a cleaved amplified polymorphism (CAP) marker digest of the PCR fragment using *PmeI* (New England Biolabs).

Approximation of endogenous BL levels

In wild type *Arabidopsis* the endogenous castasterone concentration has been reported to be 0.03-0.05 ng g⁻¹ fresh weight in roots (Bancos et al., 2002; Shimada et al., 2003). To correlate these values to a BR concentration in mol l⁻¹ the following data were used; a root of a 5-day-old seedling cut just below the hypocotyl weighs 0.18 ± 0.3 (SEM) mg (van Esse et al., 2011), and contains 95.7 ± 0.3 (SEM)% moisture. For determination of the moisture content in 5 day old seedling roots, fresh roots were weighted on pre-dried and weighted aluminium dishes (Sartorius microbalance). The samples were dried for at least 15 hours in a pre-warmed oven at 100-110 °C. To ensure that the roots did not absorb moisture after drying, roots were cooled down in a desiccator for 1 hour at room temperature. The weight of the dried roots was

determined immediately after removal from the desiccator. At least 300 roots were used for each measurement (n=5). Assuming that the ligand concentrations in a seedling root are within the same range as published (Bancos et al., 2002; Shimada et al., 2003), it was estimated that a Col-0 root of an Arabidopsis seedling contains 0.06-0.1 nM BL.

BRI1 receptor availability in Arabidopsis roots

Recently it has been reported that the BRI1-GFP receptor density in BRI1 reporter line 1 is 12 receptors μm^{-2} (van Esse et al., 2011). The BRI1-GFP reporter line contains exactly the same amount of BRI1-GFP as native BRI1 as has been demonstrated by western blot analysis (Geldner et al., 2007). Thus, this line contains in total 24 receptors μm^{-2} , when the amount of wild type receptor present is taken into account. Using this data, three different lines with three different receptor concentrations are available, the Col-0 line containing 12 receptors μm^{-2} , BRI1-GFP line 1 with 24 receptors μm^{-2} , and BRI1-GFP line 2 containing 44 receptors μm^{-2} . This corresponds to a concentration of respectively 62 nM, 120 and 200 nM BRI1, taking into account BRI1 receptors at the plasma membrane and in the endosomal vesicles close to the plasma membrane. It was assumed that the total BRI1 concentration in the hypocotyl is similar to that in the root.

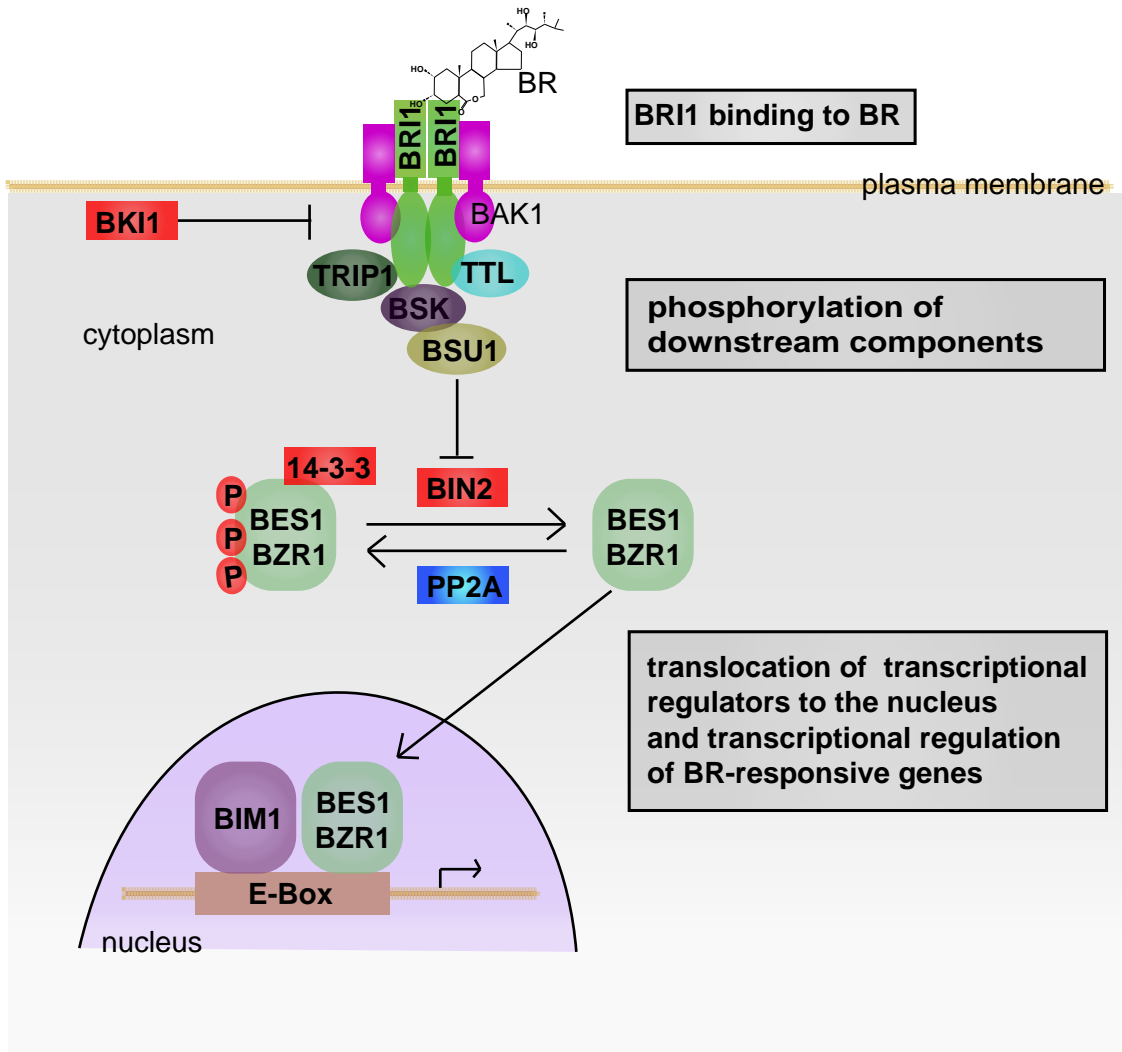


Figure S1. Schematic representation of BRI mediated BR signaling. Binding of BR to the BRI1 receptor results in the dissociation of BKI. Subsequently, BRI1 phosphorylates and activates BAK1 resulting in phosphorylation of downstream targets such as BSKs, Arabidopsis TGF- β receptor-interacting protein-1 (TRIP-1) and transthyretin-like protein (TTL). The phosphorylated BSKs enable interaction with BSU1, that inhibits BIN2 kinase while PP2A dephosphorylates BZR1 and possibly BES1. This cascade results in the accumulation of dephosphorylated BES1/BZR1 in the nucleus, where they can interact with other transcriptional regulators (e.g. BES1-interacting Myc-like 1; BIM1) to regulate the expression of various BR responsive genes. Model according to Ye et al, 2011.

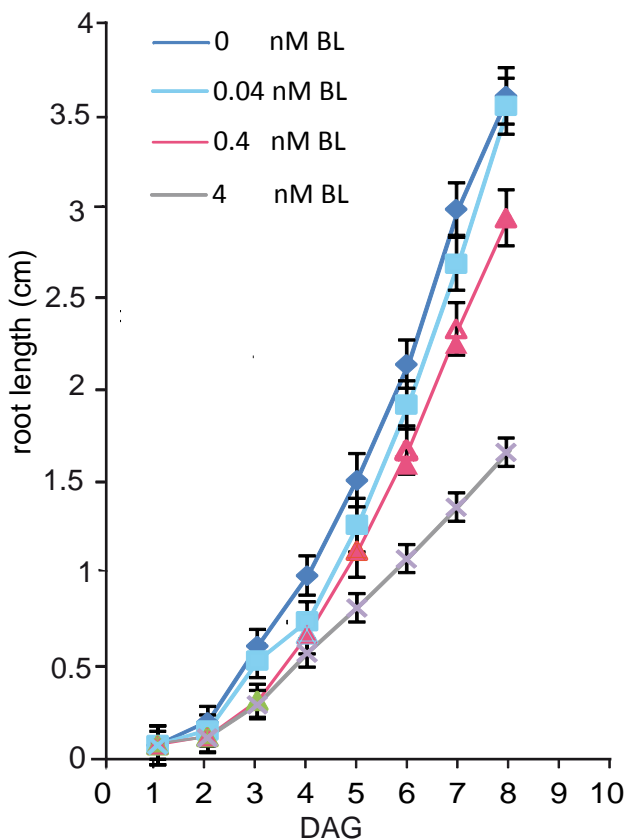
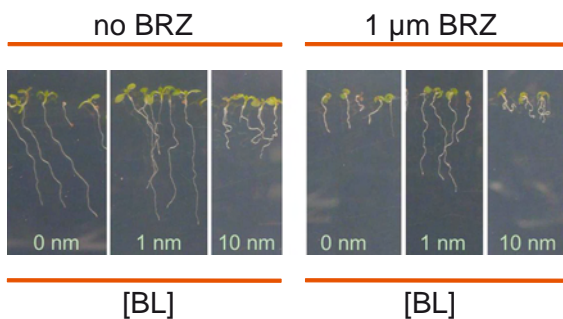
A**B**

Figure S2. Root length assay on Col-0 lines in the absence of BRZ. (A) Difference in growth in days after germination (DAG) of Col-0 seedlings after application of various concentrations BL. The stimulatory effect of BL is hard to visualize when BRZ, a biosynthetic inhibitor for BRs, is not added to the medium. (B) Seedlings treated with BL (left panel) or BL and BRZ (right panel). Representative roots are shown at 8 DAG. After application of BRZ, a clear stimulatory effect of BL on root growth is observed.

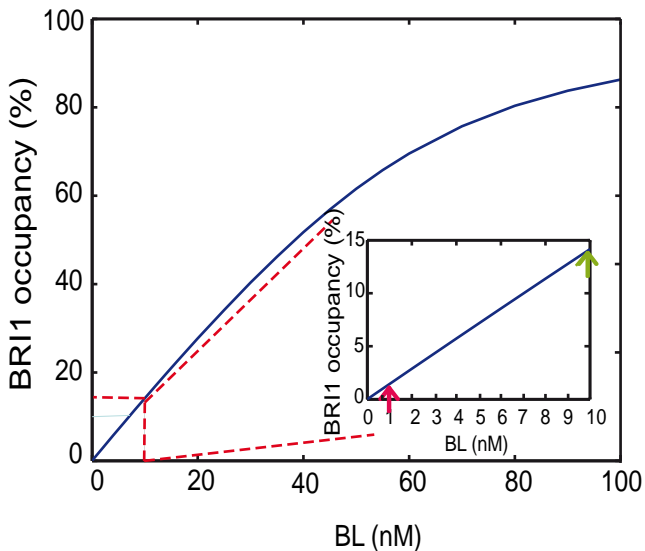


Figure S3. BRI1 receptor occupancy levels at physiological ligand concentration. At root growth stimulatory ligand concentrations around 1 nM the BRI1 receptor occupancy is less than 1% (indicated by the red arrow). The root growth is completely inhibited at a BL level of 10 nM. At this concentration around 14% of the total number of BRI1 receptors is occupied (green arrow).

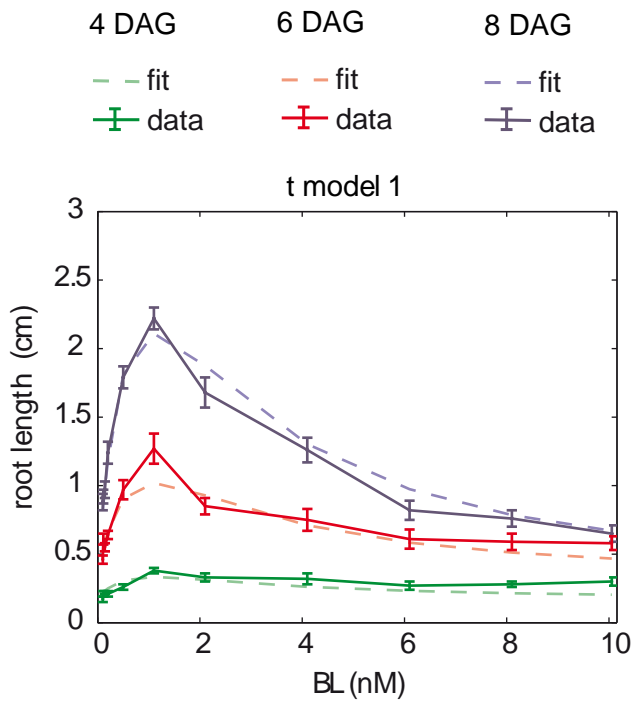
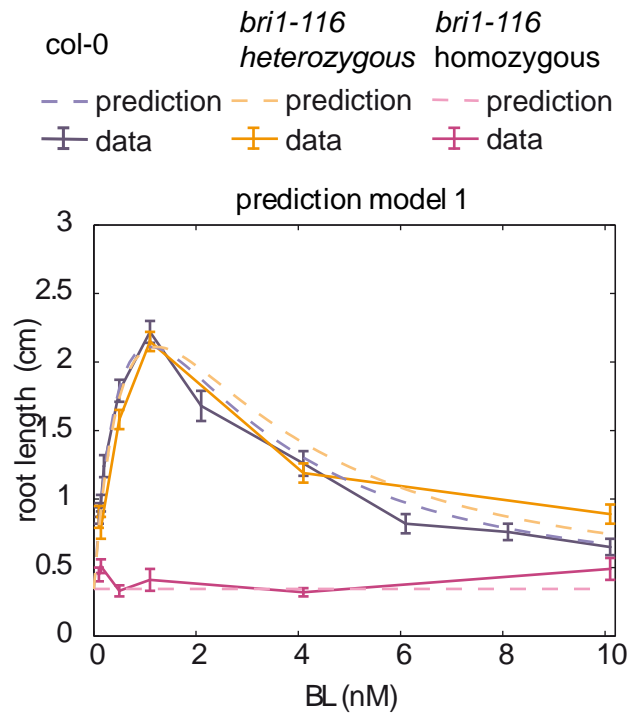
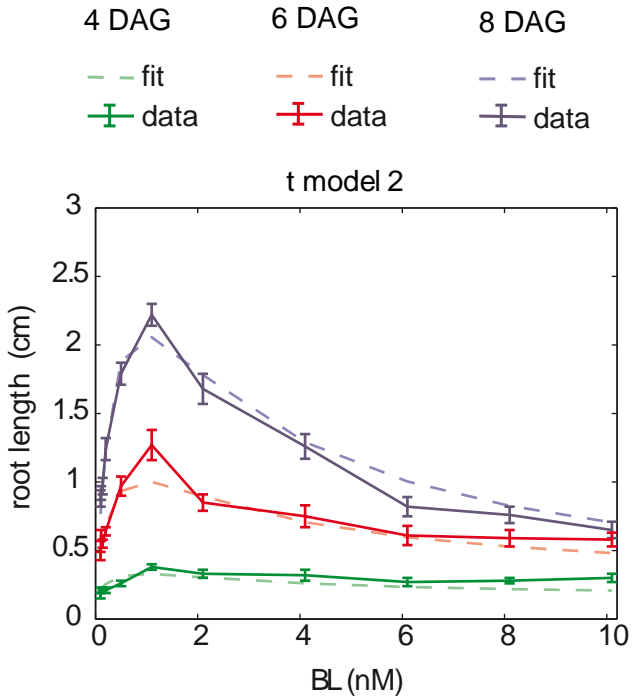
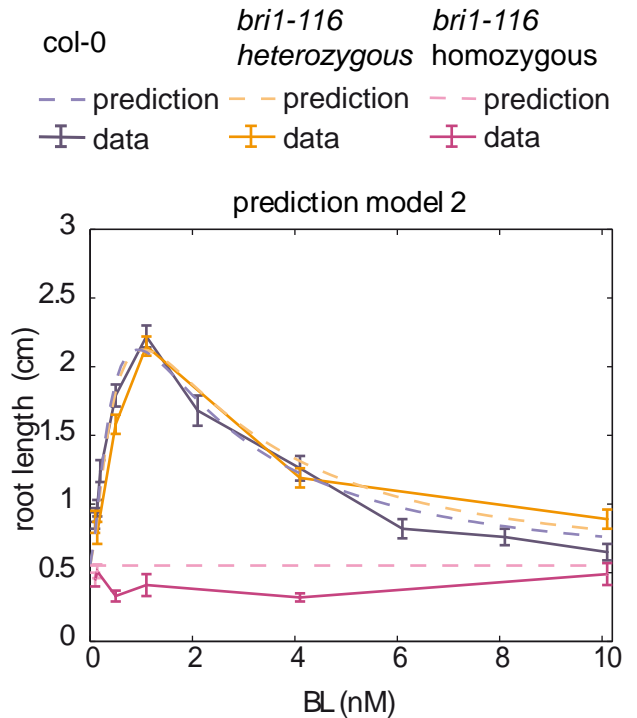
A**B****C****D**

Figure S4. Model fit and predictions model number 1 and 2. Fit of model 1(A) and 2 (C) to the root length of seedlings at 4, 6 and 8 days after germination. Model 1 consist of one stimulatory module and two inhibitory modules, model 2 has two stimulatory modules and one inhibitory module. (B and D) Model 1 (B) gives a reliable prediction of the root length at 8 DAG of *bri1-116* null mutants and *bri1-116* heterozygous lines whereas model 2 (D) prectes a slightly higer value.

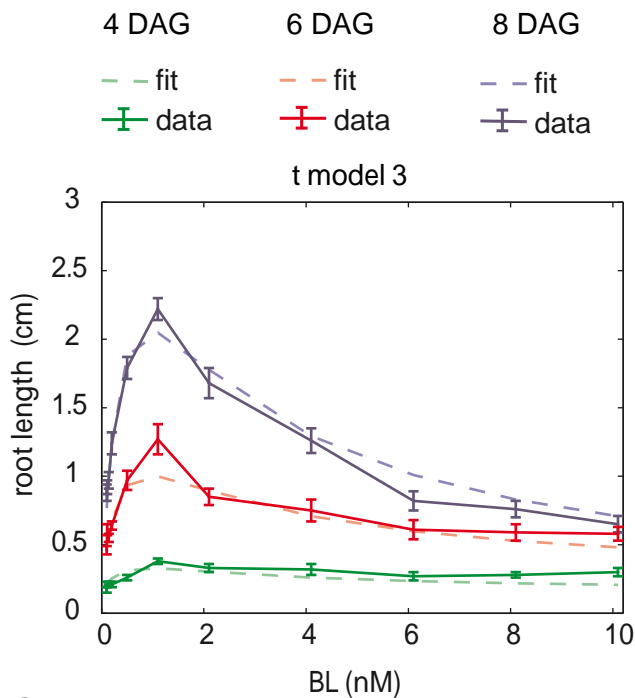
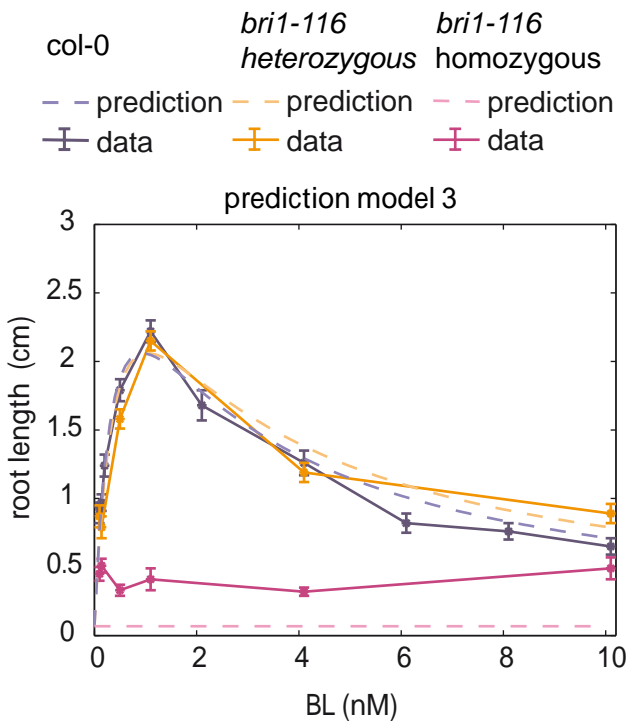
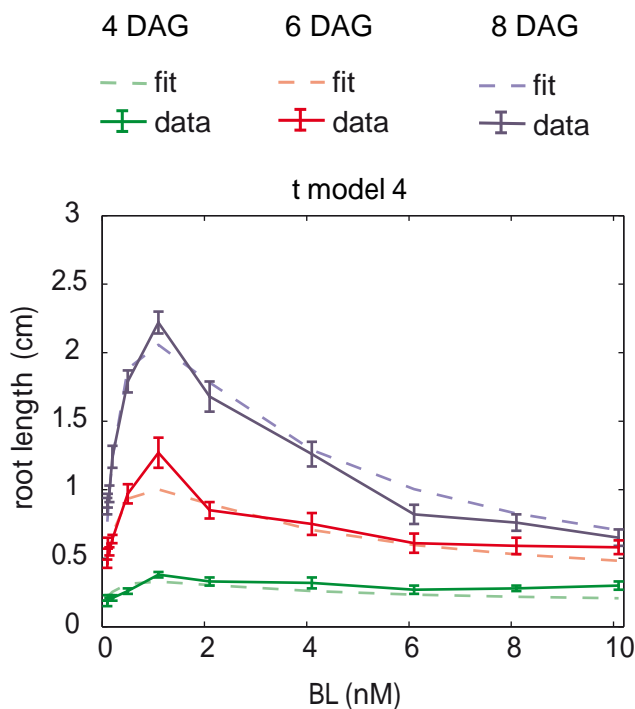
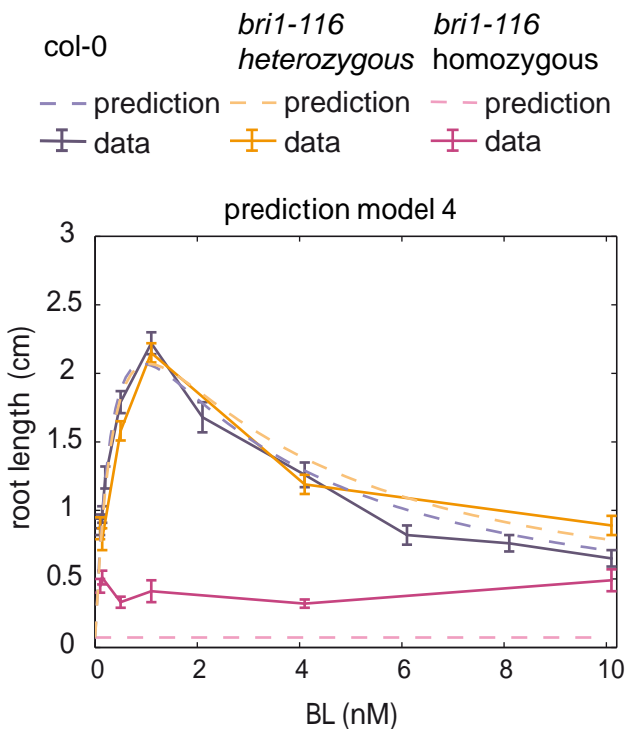
A**B****C****D**

Figure S5. Model fit and predictions model number 3 and 4. Fit of model 3(A) and 4 (C) to the root length of seedlings at 4, 6 and 8 days after germination Model 3 consist of two stimulatory modules and one inhibitory module, model 4 has one stimulatory module and one inhibitory module. Models 3 (B) and 4 (D) give a reliable prediction of the root length at 8 DAG of *bri1-116* heterozygous lines. The root length of *bri1-116* null mutants at 8 DAG could not be predicted with models 3 and 4.

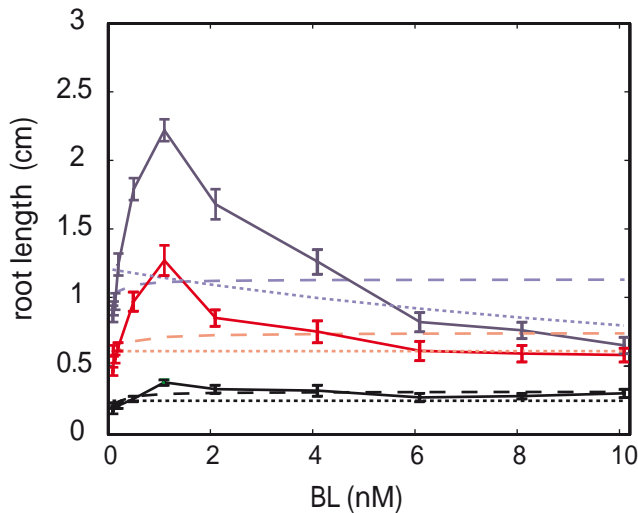
A

4 DAG 6 DAG 8 DAG

— fit model 5 - - fit model 5 - - fit model 5

..... fit model 6 fit model 6 fit model 6

—■— data -■- data -■- data

**B**

Col-0 *bri1-116*
homozygous

— prediction model 5 - - prediction model 5

..... prediction model 6 prediction model 6

—■— data -■- data

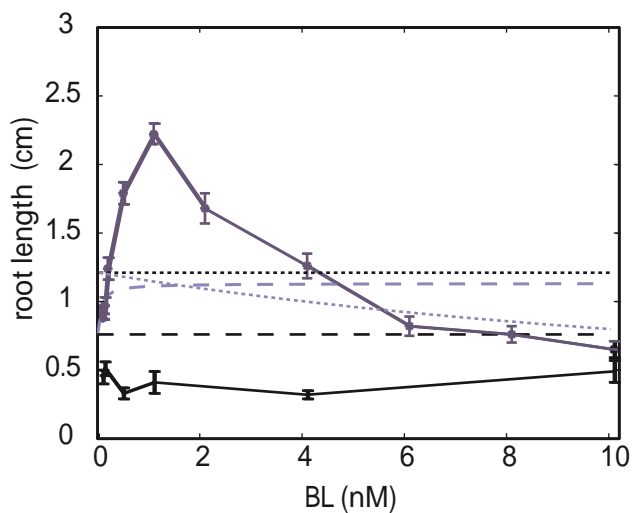
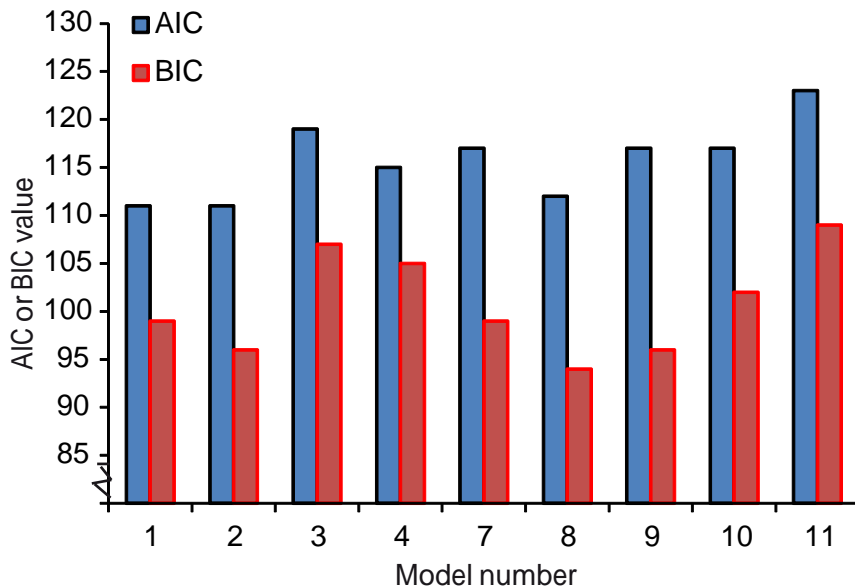
**C**

Figure S6. Modeling stimulation as well as inhibition is essential for a good fit and prediction of root length. (A) Fit of models 5 and 6 to the root length of seedlings at 4, 6 and 8 days after germination (DAG). Model 5 consist of one stimulatory module, model 6 has one inhibitory module. (B) Neither model 5 nor model 6 were able to predict the root length of wild type Col-0, *bri1-116* null mutants and *bri1-116* heterozygous lines. (C) Akaike information criterion (AIC) and the Bayesian information criterion (BIC) values when models 1-4 and 7-11 are fitted to root length of seedlings at 4,6 and 8 DAG.

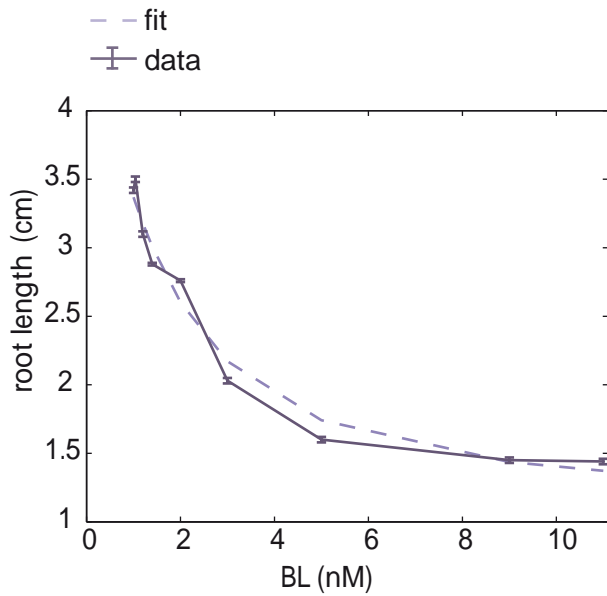


Figure S7. Fit between model 1 and Col-0 after BL stimulation in the absence of BRZ. Fit between the model and experimental data set assuming an endogenous BR level of 1 nM BL. Error bars \pm SEM; n=15 root measured in three independent replicas.

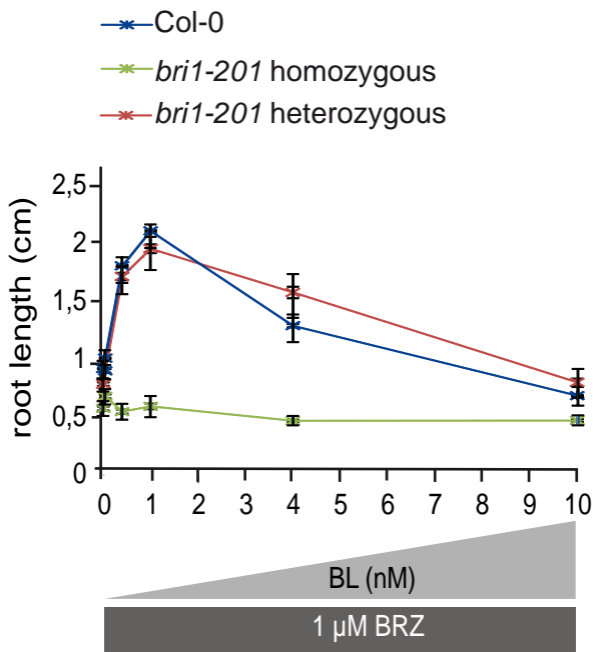


Figure S8. Root length assays on heterozygous and homozygous *bri1-201* null mutants.

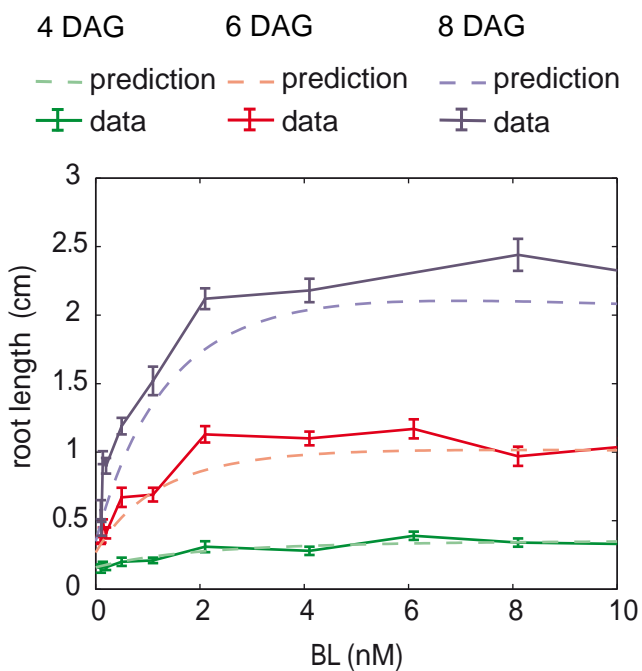
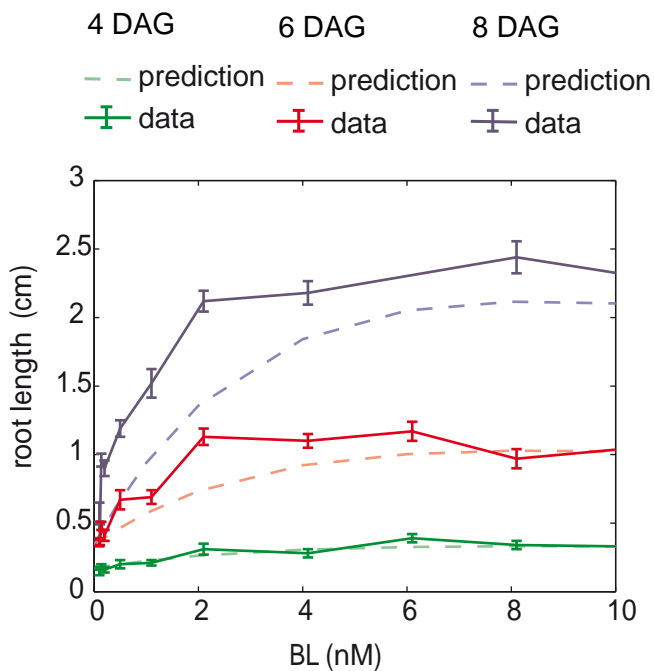
A**B**

Figure S9. Root length of *bri1-301* at 4 and 6 and 8 days after germination. (A) Model predictions versus experimental data at 4, 6 and 8 days after germination. The model is calibrated on Col-0 lines. Prediction of the *bri1-301* line is done by assuming that the total number of BRI1 receptors actively signaling is 2 nM. (B) Similar results as in (A) are obtained when the half maximum response values, k_1 , k_2 and k_3 are increased to 15 nM.

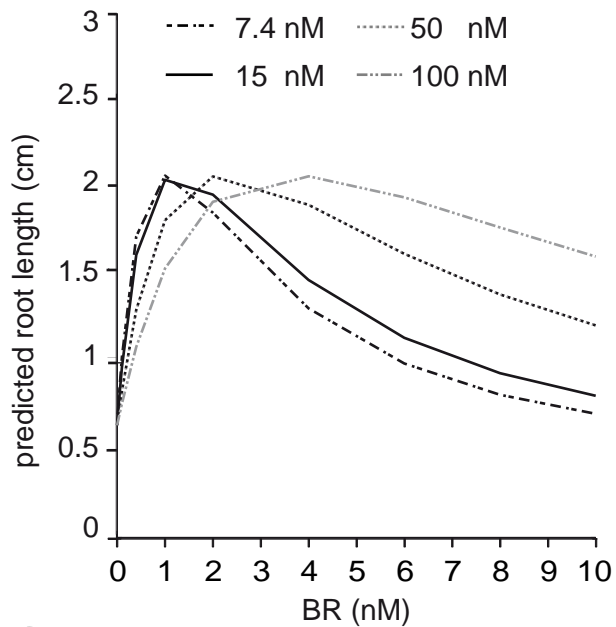
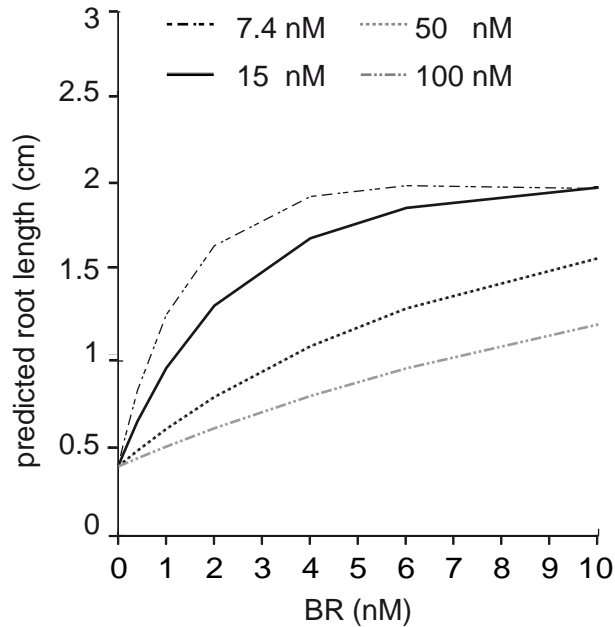
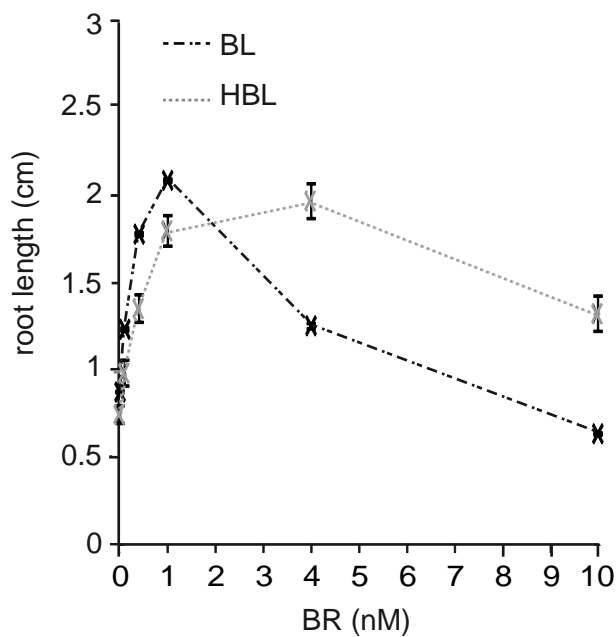
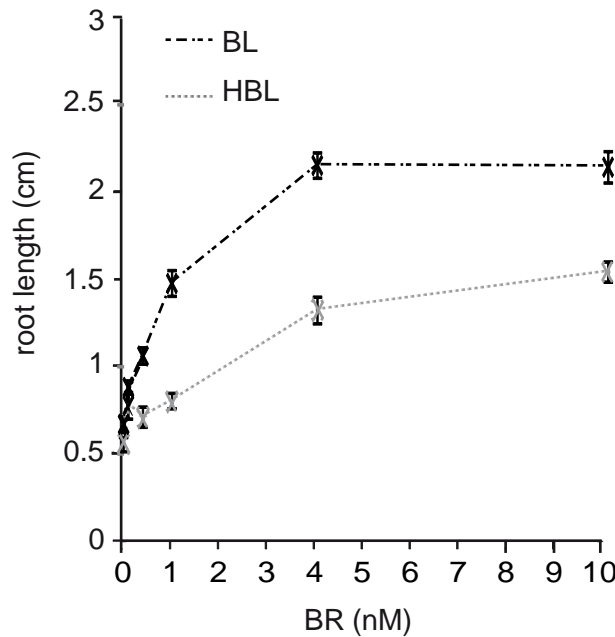
A**B****C****D**

Figure S10. Model predicts root growth in response towards less potent ligand. (A and B) The root growth of 8-day old Col-0 (A) and *bri1-301* (B) seedlings when stimulated with a less potent ligand as predicted by in silico experiments. The K_d is altered from 7.4 till 100 nM. (C and D) Actual root growth when Col-0 (C) or *bri1-301* (C) roots are grown on the less potent ligand HBL compared to root growth on BL. Error bars \pm SEM, $n = 20$ roots per data point, measured in three independent replicates.

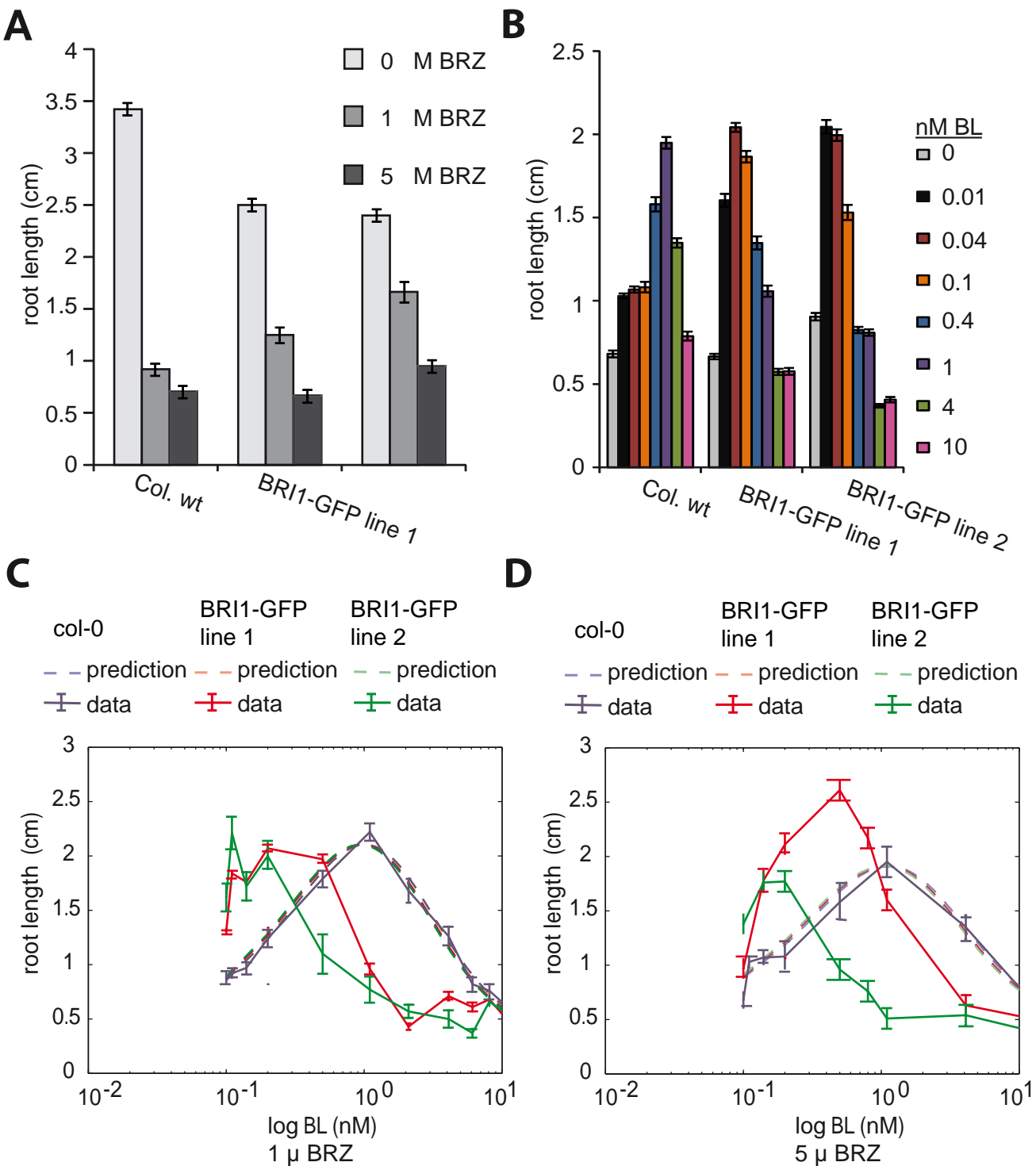


Figure S11. Root growth assays on BRI1-GFP reporter lines in presence of 5 μ M BRZ. (A) BRI1-GFP reporter lines are less sensitive towards BRZ when compared to Col-0. (B) In the presence of 5 μ M BRZ the BRI1-GFP reporter lines remain hypersensitive to BL, causing a rapid increase in root length at 0.04 nM BL (BRI1-GFP line 1) and 0.01 nM BL (BRI1-GFP line 2) after which the effect of BL on the root length is strongly inhibitory. (C and D) Fit of the model on the BRI1-GFP reporter lines when the assay is performed on 1 μ M BRZ (C) and 5 μ M BRZ (D).

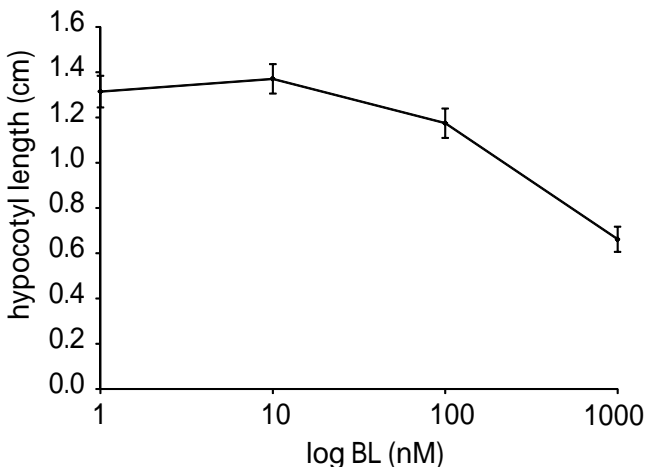
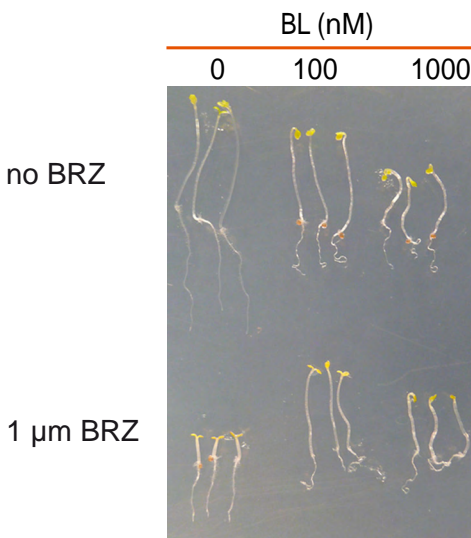
A**B**

Figure S12. Hypocotyl length assay using Col-0 when there is no BRZ in the medium. (A) Difference in hypocotyl length after application of various concentrations BL. Seedlings were grown for 5 days in the dark. Error bars \pm SEM, $n \geq 15$ hypocotyls per data point, measured in three independent replicates. (B) Seedlings treated with BL (top panel) or BL and BRZ (bottom panel). Representative hypocotyls are shown at 5 days growth in the dark. After application of BRZ, a clear stimulatory effect of BL on hypocotyl growth is observed.

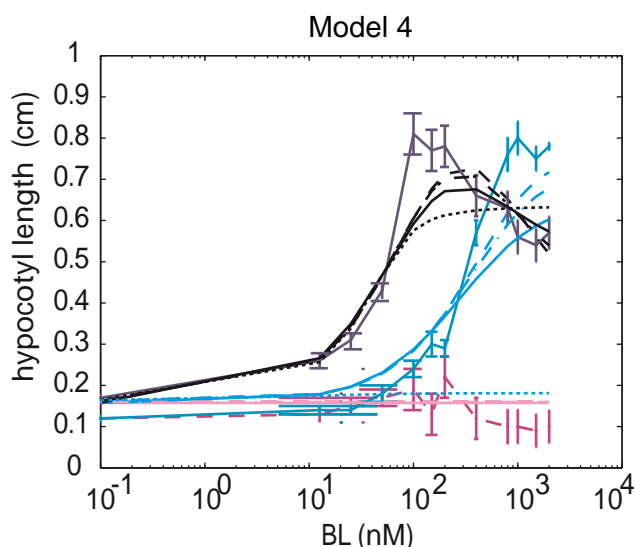
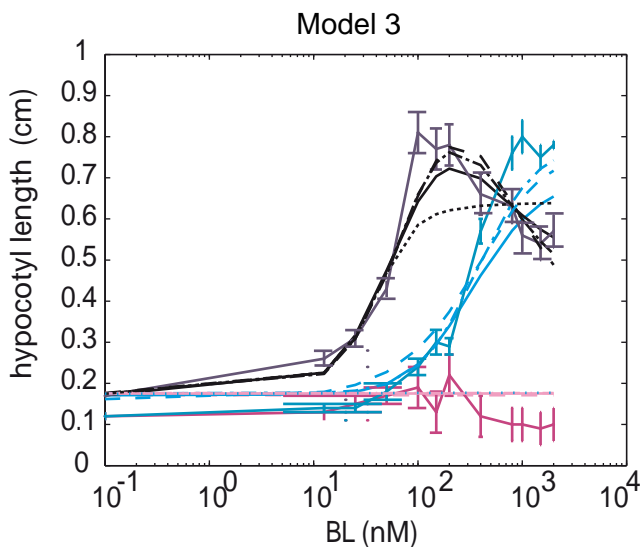
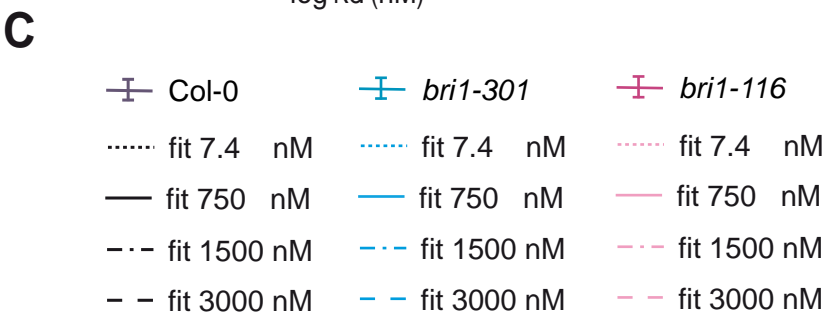
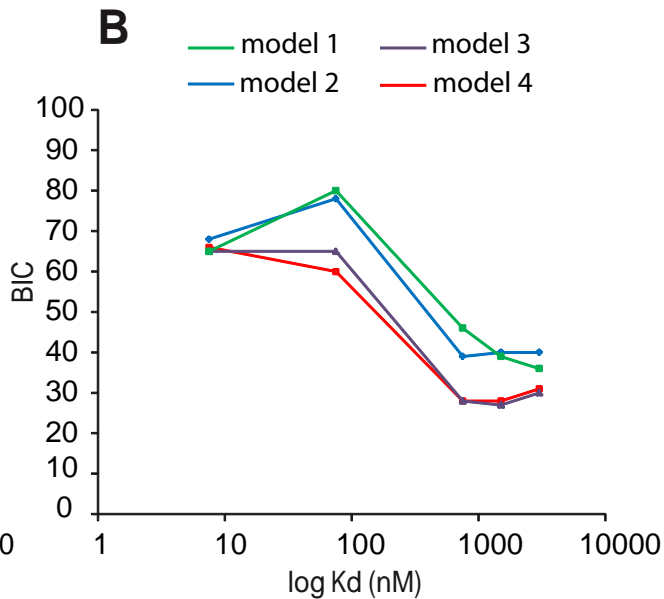
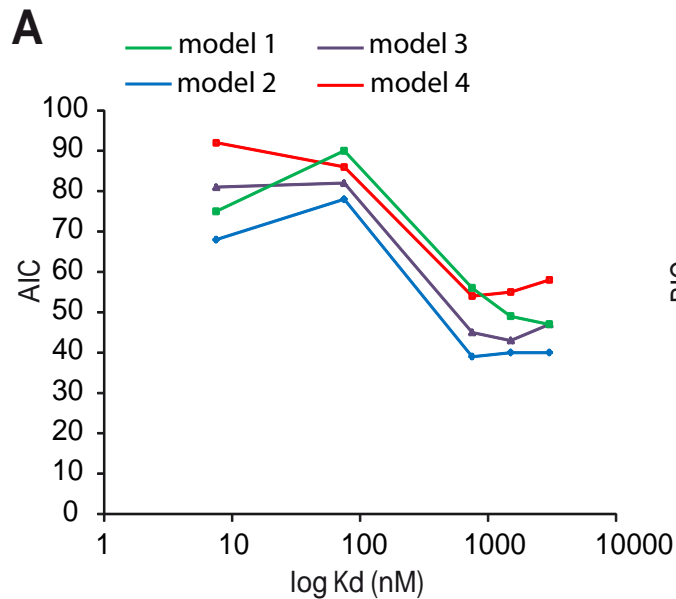


Figure S13. Model fit and predictions on hypocotyl length. (A and B) Akaike information criterion (A) and the Bayesian information criterion (B) when model structures 1-4 are fitted on hypocotyl length. The best fit is obtained for model structures 3 and 4 when increasing the Kd to at least 750 nM. (C and D) Fits of model 3 (C) and 4 (D) under varying Kd values.

Table S1. Comparison between different model structures using root length as readout.

Model nr.	Modules		S(θ^*)	AIC	BIC	Predicted root length <i>bri1-116</i> null mutant at 8 DAG (cm)
	Stimulatory	Inhibiting				
1	1	2	85	111	99	0.35
2	2	2	81	111	96	0.61
3	2	1	93	119	107	0.08
4	1	1	93	115	105	0.07
5	1	0	533	552	544	0.76
6	0	1	641	659	651	1.1
7	3	2	82	117	99	0.64
8	2	3	77	112	94	0.67
9	3	3	78	117	96	0.69
10	1	3	87	117	102	0.44
11	3	1	93	123	109	0.08

*Calibration was done on root length of seedlings at 4, 6 and 8 days after germination (DAG). Prediction of the root length of *bri1-116* null mutant was done for roots at 8 DAG. The actual root length of a *bri1-116* null mutant at 8 DAG is 0.45 ± 0.05 cm (n=15 roots, value \pm SEM).

* AIC= Akaike information criterion

* BIC= Bayesian information criterion

* S(θ^*) = least sum of squared errors

Table S2. Comparison between CRS and Matlab genetic algorithm (GA) combined with Isqnonlin.

	4 DAG		6 DAG		8 DAG	
	CRS	GA+ Isqnonlin	CRS	GA+ Isqnonlin	CRS	GA+ Lsqnonlin
E_{max} (cm)	1.05±0.08	1.07±0.01	4.60±0.26	4.55±0.01	12.21±0.85	11.90±0.05
R (0,0,t) (cm)	0.18±0.01	0.18±0.00	0.35±0.13	0.34±0.00	0.35±0.00	0.35±0.00
k₁	2.03±0.16	1.97±0.00				
k₂	1.95±0.08	1.98±0.01				
k₃	1.96±0.13	1.98±0.00				

*Values ±STDEV, n= 5 runs

* R(0,0,t) =the root length at time 0 in the absence of BRI1 mediated signalling

* E_{max} =the maximum possible root length when no inhibitory mechanisms are present

* k₁,k₂ and k₃ are the half maximum response values

* CRS= controlled random search

* GA + Isqnonlin= Matlab genetic algorithm followed by Isqnonlin

Table S3. Comparison between different model structures using hypocotyl length as readout.

Model nr.	Modules		S(θ^*)	AIC	BIC	Predicted root length <i>bri1-116</i> null mutant at 8 DAG (cm)
	Stimulatory	Inhibiting				
1	1	2	30	52	35	0.16
2	2	2	22	55	28	0.18
3	2	1	22	44	27	0.18
4	1	1	34	49	38	0.16
5	1	0	92	101	95	0.16
6	0	1	738	747	741	0.32
7	3	2	22	73	29	0.18
8	2	3	22	74	30	0.18
9	3	3	22	110	31	0.18
10	1	3	30	63	37	0.16
11	3	1	22	55	28	0.18

* Calibration was done on hypocotyl length of seedlings grown for 5 days in the dark. The actual hypocotyl length of a *bri1-116* null mutant grown for 5 days in the dark is 0.14 ± 0.01 cm (n=15 hypocotyls, value \pm SEM).

* AIC= Akaike information criterion

* BIC= Bayesian information criterion

* S(θ^*) = least sum of squared errors